Chemical Physics Letters 509 (2011) 72–76

Contents lists available at ScienceDirect

Chemical Physics Letters

journal homepage: www.elsevier.com/locate/cplett

Monitoring potassium metal electrodeposition from an ionic liquid using *in situ* electrochemical-X-ray photoelectron spectroscopy

Rahmat Wibowo [a], Leigh Aldous [a], Robert M.J. Jacobs [b], Ninie S.A. Manan [c,d], Richard G. Compton [a,*]

[a] *Department of Chemistry, Physical and Theoretical Chemistry Laboratory, University of Oxford, South Parks Road, Oxford OX1 3QZ, United Kingdom*
[b] *Department of Chemistry, Chemistry Research Laboratory, University of Oxford, Mansfield Road, Oxford OX1 3TA, United Kingdom*
[c] *School of Chemistry and Chemical Engineering, The QUILL Centre, Queen's University Belfast, Belfast BT9 5AG, United Kingdom*
[d] *Department of Chemistry, Faculty of Science, University of Malaya, 50603 Kuala Lumpur, Malaysia*

ARTICLE INFO

Article history:
Received 10 April 2011
In final form 22 April 2011
Available online 28 April 2011

ABSTRACT

The real time electrodeposition of potassium has been monitored for the first time in an ionic liquid using *in situ* electrodeposition-X-ray photoelectron spectroscopy (XPS). The ionic liquid used was *N*-butyl-*N*-methylpyrrolidinium bis(trifluoromethylsulfonyl)imide ($[C_4mpyrr][NTf_2]$), and electrodeposition occurred at a nickel mesh electrode. Potassium electrochemistry was monitored at the ionic liquid–vacuum–electrode interface using a novel cell design.

1. Introduction

Ionic liquids (ILs) generally possess extremely low vapour pressures [1], as well as inherent conductivity and the ability to support relatively reactive metal deposits [2]. These characteristics have facilitated their application in a number of relatively unique *in vacuo* techniques [3,4], including *in situ* X-ray photoelectron spectroscopy (XPS) of ionic liquids and various solutes [3,5–22]. This has recently been expanded to *in situ* electrochemical-XPS measurements, a form of *in vacuo* spectroelectrochemical measurement [9,22–24].

Foelske-Schmitz et al. investigated the electrochemistry of Highly Orientated Pyrolytic Graphite (HOPG) in the ionic liquid $[C_4mim][BF_4]$, which was performed in the XPS chamber, the excess liquid removed from the carbon surface, the carbon transferred to the sample holder and XPS performed [9]. Silvester performed XPS measurements in conjunction with *ex situ* electrochemical measurements in order to probe the bromide content of $[C_4mpyrr][NTf_2]$ [20].

Licence et al. have carried out *in situ* electrochemical-XPS measurements using two-electrode systems containing IL droplets, and monitored the oxidation of a copper wire to Cu(I) [23], reduction of Fe(III) to Fe(II) [24] and the XPS induced charging of the IL itself [22].

Weingarth et al. have also recently accomplished *in situ* electrochemical-XPS measurements, whereby the X-ray beam was focused on the interface between the IL and a Pt electrode, a potential difference applied and spectra recorded at the polarised interface; this represented the first, and to the authors knowledge only reported application to date of a three-electrode electrochemical set-up for *in situ* electrochemical-XPS measurements on ILs [25].

We have recently investigated the electrodeposition of the Alkali Group I metals at Pt and Ni electrodes in the IL *N*-butyl-*N*-methylpyrrolidinium bis(trifluoromethylsulfonyl)imide ($[C_4mpyrr][NTf_2]$), allowing determination of a range of fundamental kinetic and thermodynamic properties [26–29]. These metals are of particular interest with regards to energy storage devices such as batteries, and our work highlights the similarity in the trends within the Alkali metal group with $[C_4mpyrr][NTf_2]$ and the common battery electrolyte propylene carbonate. The tendency of these metals to form dendritic electrodeposits is of both interest and concern, as it can result in harmful short-circuiting of battery devices [30].

In this Letter we report for the first time *in situ* metal electrodeposition-XPS measurements in an ionic liquid, achieved with a unique cell design which allowed real time measurement of potassium metal electrodeposition from $[C_4mpyrr][NTf_2]$ at the three-phase ionic liquid–electrode–vacuum boundary.

2. Experimental

N-Butyl-*N*-methylpyrrolidinium bis(trifluoromethylsulfonyl)-imide ($[C_4mpyrr][NTf_2]$) was prepared in-house using standard methods [31]. The $K[NTf_2]$ salt was prepared by the reaction of aqueous solutions of the appropriate potassium hydroxide salt with a 5% molar excess of $H[NTf_2]$, followed by repeated dissolution in water then drying under vacuum, until pH neutral.

XPS measurements were performed using a VG ESCALAB MkII spectrometer equipped with a monochromatic Al Kα X-ray source (photon energy of 1486.6 eV). All XPS experiments were recorded

---

[*] Corresponding author. Fax: +44 0 1865 275 410.
E-mail address: richard.compton@chem.ox.ac.uk (R.G. Compton).

0009-2614/$ - see front matter © 2011 Elsevier B.V. All rights reserved.
doi:10.1016/j.cplett.2011.04.071

with a constant analyser pass energy of 100 eV for survey scans and 20 eV for detailed scans. All XPS spectra were referenced to the cations C 1s peak, using a binding energy of 285.0 eV. The cell was covered with a specially fashion lid to prevent ionic liquid loss during degassing, placed upright in a desiccator and put under high vacuum overnight before use. The cell was then rapidly transferred to the entry chamber and evacuated for a further 2 h before being moved into the sample chamber.

All electrochemical measurements were carried out using a computer-controlled PGSTAT-12 μ-Autolab potentiostat (Eco-Chemie, Netherlands).

3. Results and discussion

3.1. Experimental set-up

A custom electrochemistry-XPS cell and cell holder were fabricated in house, and are depicted in Figure 1. The cell consisted of two hollow cylinders of PEEK, as well as a modified stainless steel XPS stub. These pieces were precisely machined and then firmly pressed together. A shallow well ca. 1 mm deep was made across the surface of the top cylinder of PEEK, and the hollow cylinder and shallow well filled with IL (ca. 150 μl). Two pieces of copper foil were sandwiched between the two cylinders of PEEK, and two tapered holes drilled into the bottom cylinder of PEEK. One piece of foil was joined to a Pt wire, which was brought into contact with the IL to act as a quasi-reference electrode (depicted as ‘a’ in Figure 1). The second piece of foil was joined to a Ni mesh via a Pt wire to act as working electrode (b). This mesh was allowed to float on the surface of the IL, forming a three-phase boundary between the IL, Ni and vacuum. The stainless steel stub (c) was used as counter electrode. A removable lid was fashioned to prevent loss of the IL during its vigorous bubbling when initially *in vacuo*.

Electrical connection from the potentiostat to the cell was provided by a removable cell holder. This cell holder was moved around and anchored in place in a traditional cell holder by a modified XPS stub on the underside (g), allowing electrochemical measurements to be performed in addition to traditional samples. The cell was lowered from above onto two pogo spring pins (d and e), which entered the tapered holes and made electrical contact with the working and reference electrodes, respectively, via the copper foil. Much of the counter electrode (c) passed through a hole in the holder before coming to rest on a copper o-ring set in the holder (f). Three shielded wires (from d to f) ran from the holder to the potentiostat, via an electrical feed-through in the XPS housing.

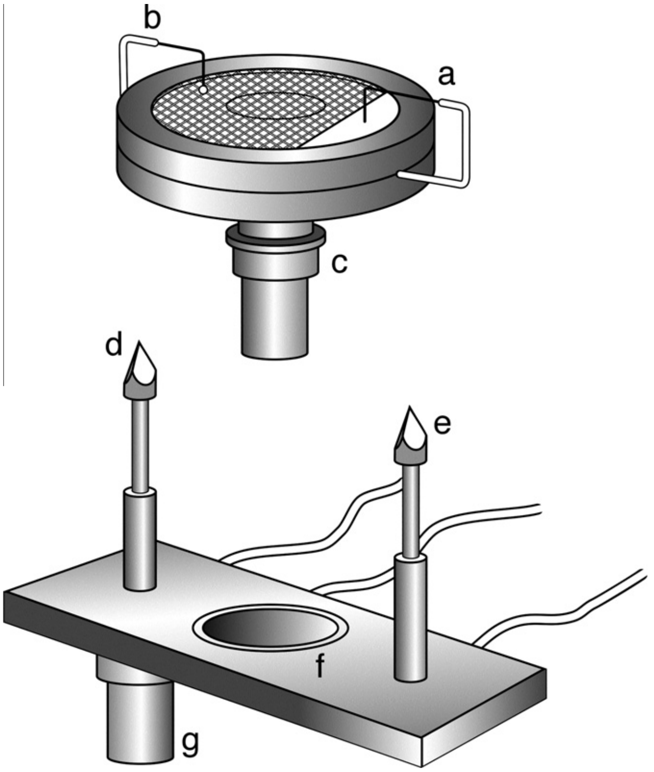

Figure 1. *In situ* XPS-electrochemical cell and associated holder.

3.2. XPS measurement

XPS spectra of the electrochemical set-up was recorded, and Figure 2 displays a wide scan for both 0.1 M and 0.5 M K[*N*Tf$_2$] dissolved in [C$_4$mpyrr][*N*Tf$_2$]. Clear signals were observed for the IL, corresponding to C, N, O, F and S. The stoichiometric ratios agreed well (within ca. 5%) of those expected for the pure IL. Signals for K 2p and K 2s at 295 and 377 eV were not observed for solutions containing 0.1 M K[*N*Tf$_2$], but could be observed for 0.5 M K[*N*Tf$_2$].

In both spectra only weak signals were observed for Ni 2p$_{3/2}$ at 855 eV, despite the presence of a significant quantity of Ni in the form of the Ni mesh. The weak signal was found to be related to the angle of the sample with respect to the detector. The sample was kept horizontal when the cell contained IL, with a corresponding take off angle of 75°. This resulted in strong signals for the surface of the IL, but could only detect the top surface of the Ni mesh, emission from the side of the Ni mesh being largely unable to reach the detector. Tilting the sample to change the take off angle to 90° (e.g. with the mesh adhered to a carbon tab) resulted in a significant increase in the Ni signal. However, measurement at this angle was not possible when IL was present in the cell, and it is also noted that analysis of the Ni mesh was not required, interest instead being focused on the surface of the IL in the vicinity of the Ni mesh.

3.3. Cyclic voltammetry performed in the XPS chamber

Figure 3 displays cyclic voltammetry recorded for 0.5 M K[*N*Tf$_2$] in [C$_4$mpyrr][*N*Tf$_2$] in the *in situ* electrochemical-XPS cell, scanning at 10 mV s^{-1} between 0 and −3.6 V vs. Pt wire. The observed response bears strong resemblance to the previously reported data

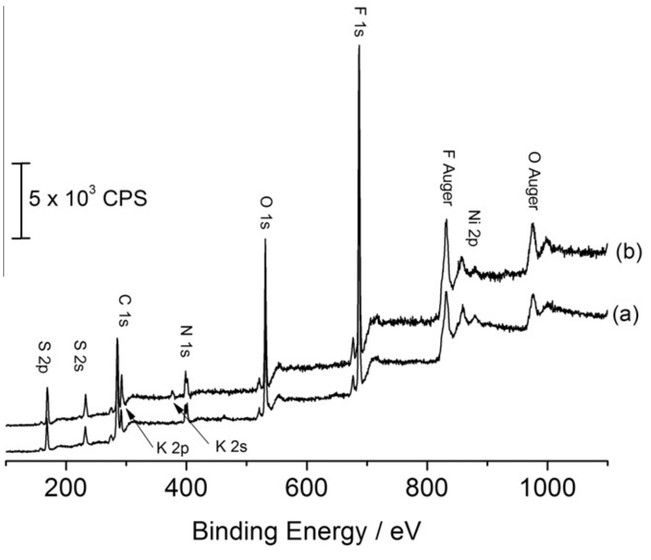

Figure 2. X-ray photoelectron spectra recorded for the *in situ* electrochemistry-XPS cell when filled with (a) 0.1 M K[*N*Tf$_2$] and (b) 0.5 M K[*N*Tf$_2$] in [C$_4$mpyrr][*N*Tf$_2$].

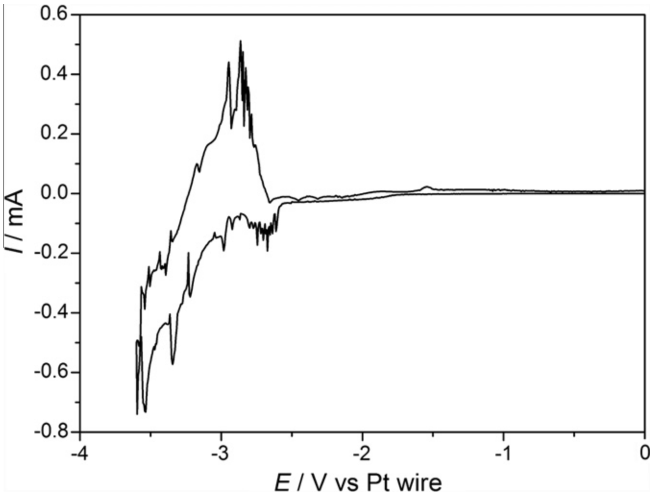

Figure 3. Cyclic voltammogram recorded for 0.5 M K[NTf$_2$] in [C$_4$mpyrr][NTf$_2$] at a Ni mesh electrode inside the XPS chamber. Scan rate = 10 mV s^{-1}.

recorded under similar conditions at a Ni microdisk electrode [26], namely K underpotential deposition features occurring in the region of ca. −1.5 to −2.5 V with bulk electrodeposition of K metal from ca. −3 V onwards. Stripping of the bulk metal deposit is observed on the reverse scan. Stripping efficiency was less that 100% on the Ni mesh (ca. 33% efficiency in Figure 3), which has been previous noted for K on Ni microdisk electrodes [26], as well as for a range of other metals on a range of substrates [32]. If this low stripping efficiency was due to reaction of K metal with trace impurities present in the IL, stripping efficiency would decrease as the concentration of K[NTf$_2$] decreased (due to a higher ratio of possible reactants to K electrodeposited). However, experiments at a Ni microdisk electrode demonstrated that a maximum striping efficiency was observed at ca. 0.1 M K[NTf$_2$] and stripping efficiency decreased with increasing K[NTf$_2$] concentration, therefore this trend can tentatively be assigned to dendritic metal deposits forming. During oxidation the material in contact with the electrode is oxidised first, and the remainder loses good electrical contact with the electrode resulting in less than 100% stripping efficiency [32].

3.4. In situ electrodeposition-XPS measurements

Electrodeposition of K metal at the Ni mesh was performed by holding the potential at −3.2 V vs. the Pt wire quasi-reference. XPS measurements were performed periodically, both in wide scan mode and by performing detailed scans in the K 2s region; attention was focused on the K 2s region as the K 2p partially overlapped with the C 1s signal from the [NTf$_2$]$^-$ anion.

For the first ca. 12 h, the K 2s region was essentially featureless (Figure 4), although with extended electrolysis time (up to 36 h) increasing quantities of K were detected at the surface of the IL, corresponding to electrodeposited K metal. From 15 h onwards the quantity of K detected was found to increase in an approximately linear manner with time (Figure 5). The preceding 15 h appeared to correspond to an induction period, likely corresponding to the formation of K electrodeposits growing on and close to the Ni surface which due to the take off angle could not be detected. After 36 h a total charge of 4.5 C was passed, corresponding to approximately 2 mg of K metal deposited (assuming 100% columbic efficiency). An electrolysis extending over 36 h is expected when dealing with IL systems, due to the relatively high viscosity and low diffusion coefficients typically experienced in IL systems. For example, the diffusion coefficient of K$^+$ in [C$_4$mpyrr][NTf$_2$] (D = 1.02 × 10^{-11} m^2 s^{-1}) [26] is two orders of magnitude slower than that observed in aqueous media (D = ca. 3 × 10^{-9} m^2 s^{-1}) [33].

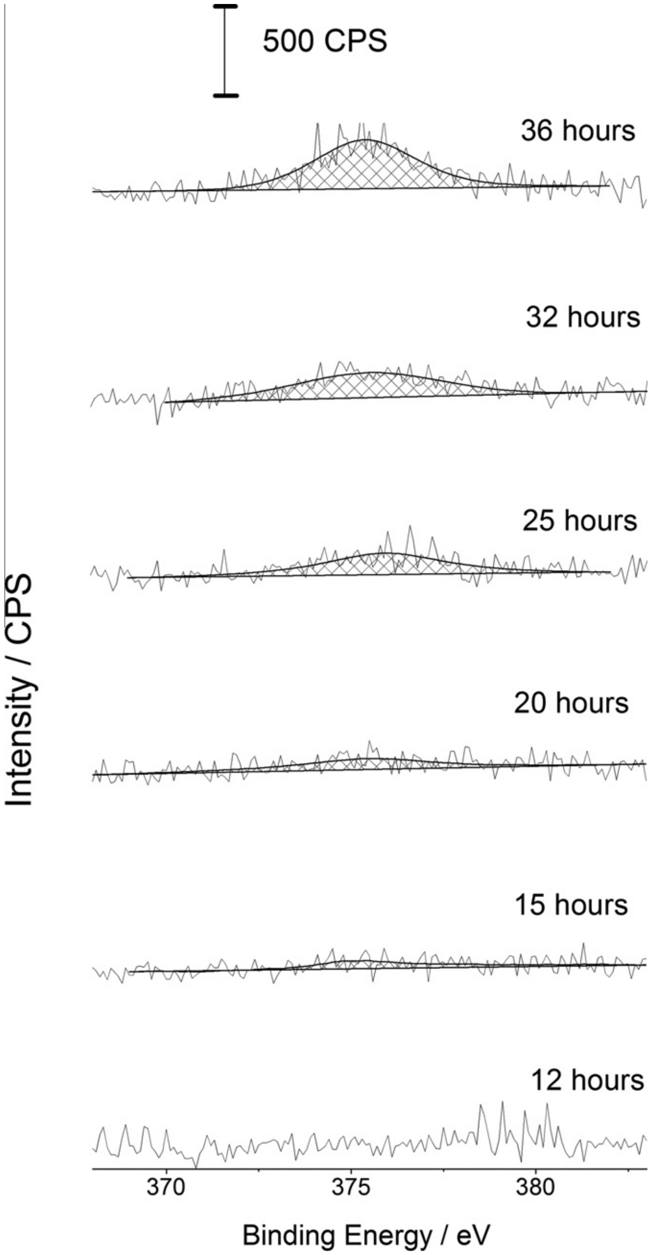

Figure 4. XPS high resolution scans (pass energy of 20 eV, 10 scans) for the K 2s region taken during electrolysis at −3.2 V vs. Pt quasi-reference at a Ni mesh electrode floating on 0.1 M K[NTf$_2$] in [C$_4$mpyrr][NTf$_2$]. The scans were recorded after 12, 15, 20, 25, 32 and 36 h of electrolysis.

After 36 h the electrolysis was ceased and all connections running from the potentiostat to the XPS unplugged. The system was allowed to remain like that for 1 h before another XPS measurement recorded. The measurement demonstrated no significant change in the various peaks relative to that recorded before electrolysis was ceased, showing that the system was stable for this period. After this the cell was reconnected, and the K deposit oxidised at an applied potential of 0 V vs. Pt wire quasi-reference for 30 min. Figure 6 displays the XPS spectra recorded (a) after holding −3.2 V for 36 h and (b) after the subsequent application of 0 V for 30 min. There is clearly a significant decrease in the size of the K peak, corresponding to oxidation of K (in contact with the Ni) to K$^+$, with much of the resulting K$^+$, as well as K metal no longer adhered to the Ni surface diffusing away.

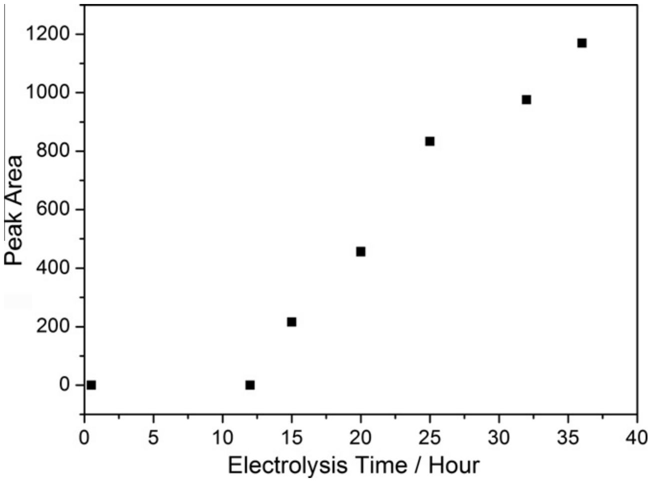

Figure 5. Plot of the absolute XPS peak area recorded under the K 2s peak as a function of electrolysis time.

3.5. Is it possible to distinguish between potassium metal and potassium ions?

During this work, it was observed that when the electrochemical cell was polarised between applied potentials of −2.0 V to +0.5 V vs. Pt quasi-reference (no Faradaic current passed), the binding energy of all elements shifted by -0.82 eV V^{-1} ($R^2 = 0.99$ for linear fit, $n = 5$) implying minor distortion of the IL-vacuum interface due to the polarised Ni mesh. This shift is distinct from the recently highlighted -1.0 eV V^{-1} 'electrochemical shift' experienced by IL molecules in the electrochemical double layer [25], as our focus was extended over an area considerably larger than the double layer. However, this was accounted for by referencing all spectra to the ionic liquid C 1s peak.

It is feasible to distinguish between K^+ ions and K bulk metal using XPS as they possess distinct binding energies, e.g. 1.2 eV difference for the K $2p_{3/2}$ peaks [34]. However, at the start of electrolysis the K^+ ions XPS peak could not be observed. During electrolysis a potassium peak developed in the XPS spectra, although the precise binding energy determined by fitting of the peak was found to shift by up to 0.8 eV. This was largely a feature of instrumental noise resulting in some ambiguity regarding the precise position of the peak. Additionally, Villar-Garcia et al. have recently highlighted that the charging of the ionic liquid surfaces during X-ray irradiation, as well as day-to-day variations can lead to binding energy values shifting by at least 0.8 eV unless internal referencing to unaffected moieties is performed (e.g. long-chain aliphatic carbon peaks) [22], which was not possible in this current work. Therefore given the minor uncertainties present, elements can be accurately identified and quantified but detailed speciation information (such as differentiation between K and K^+) cannot be accurately assigned to the system.

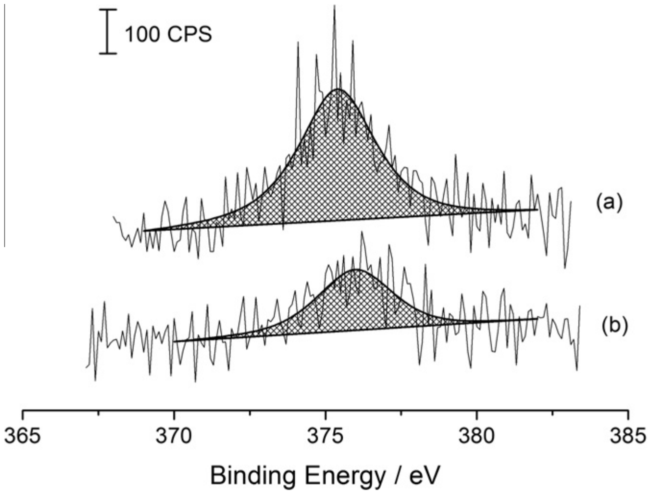

Figure 6. XPS high resolution scan for K 2s taken (a) after 36 h of electrodeposition at −3.2 V and (b) after the oxidation of the deposit for 30 min at 0 V.

4. Conclusion

A novel cell design designed for application in conventional XPS chambers has been presented. Using this design it has been clearly been demonstrated that the growth of (reactive) metal deposits can be monitored at the three-phase ionic liquid–electrode–vacuum boundary using *in situ* XPS measurements.

Acknowledgements

Professor Christopher Hardacre is thanked for the kind donation of the ionic liquid, which was synthesized by N.S.A.M. N.S.A.M. acknowledges the financial support of the Ministry of Higher Education Malaysia and University of Malaya via a SLAI fellowship. R.W. thanks the Directorate of Higher Education, The Ministry of National Education, Republic of Indonesia for funding. John Freeman is thanked for assistance with Figure 1, and Charlie Jones for the construction of the cell and holder.

References

[1] J.M.S.S. Esperanca, J.N.C. Lopes, M. Tariq, L.M.N.B.F. Santos, J.W. Magee, L.P.N. Rebelo, J. Chem. Eng. Data 55 (2010) 3.
[2] F.P.D. Endres, D. MacFarlane, A. Abbott, Electrodeposition from Ionic Liquids, Wiley-VCH, Weinheim, Chichester, 2008.
[3] E.F. Smith, F.J.M. Rutten, I.J. Villar-Garcia, D. Briggs, P. Licence, Langmuir 22 (2006) 9386.
[4] S. Kuwabata, T. Tsuda, T. Torimoto, J. Phys. Chem. Lett. 1 (2010) 3177.
[5] F. Bernardi, J.D. Scholten, G.H. Fecher, J. Dupont, J. Morais, Chem. Phys. Lett. 479 (2009) 113.
[6] J.K. Chang, M.T. Lee, W.T. Tsai, M.J. Deng, H.F. Cheng, I.W. Sun, Langmuir 25 (2009) 11955.
[7] J.K. Chang, M.T. Lee, W.T. Tsai, M.J. Deng, I.W. Sun, Chem. Mater. 21 (2009) 2688.
[8] T. Cremer et al., Chemistry-a European Journal 16 (2010) 9018.
[9] A. Foelske-Schmitz, D. Weingarth, H. Kaiser, R. Kotz, Electrochem. Commun. 12 (2010) 1453.
[10] R. Fortunato, C.A.M. Afonso, J. Benavente, E. Rodriguez-Castellon, J.G. Crespo, J. Membr. Sci. 256 (2005) 216.
[11] J.M. Gottfried, F. Maier, J. Rossa, D. Gerhard, P.S. Schulz, P. Wasserscheid, H.P. Steinruck, Zeitschrift Fur Physikalische Chemie-International Journal of Research in Physical Chemistry & Chemical Physics 220 (2006) 1439.
[12] H. Hashimoto, A. Ohno, K. Nakajima, M. Suzuki, H. Tsuji, K. Kimura, Surf. Sci. 604 (2010) 464.
[13] O. Hofft, S. Bahr, M. Himmerlich, S. Krischok, J.A. Schaefer, V. Kempter, Langmuir 22 (2006) 7120.
[14] S. Krischok et al., J. Phys. Chem. B 111 (2007) 4801.
[15] J.H. Kwon, S.W. Youn, Y.C. Kang, Bull. Korean Chem. Soc. 27 (2006) 1851.
[16] V. Lockett, R. Sedev, C. Bassell, J. Ralston, Phys. Chem. Chem. Phys. 10 (2008) 1330.
[17] K.R.J. Lovelock, I.J. Villar-Garcia, F. Maier, H.P. Steinruck, P. Licence, Chem. Rev. 110 (2010) 5158.
[18] F. Maier et al., Angewandte Chemie-International Edition 45 (2006) 7778.
[19] M. Shigeyasu, H. Murayama, H. Tanaka, Chem. Phys. Lett. 463 (2008) 373.
[20] D.S. Silvester, T.L. Broder, L. Aldous, C. Hardacre, A. Crossley, R.G. Compton, Analyst 132 (2007) 196.
[21] E.F. Smith, I.J. Villar Garcia, D. Briggs, P. Licence, Chem. Commun. (2005) 5633.
[22] I.J. Villar-Garcia, E.F. Smith, A.W. Taylor, F.L. Qiu, K.R.J. Lovelock, R.G. Jones, P. Licence, Phys. Chem. Chem. Phys. 13 (2011) 2797.
[23] F.L. Qiu, A.W. Taylor, S. Men, I.J. Villar-Garcia, P. Licence, Phys. Chem. Chem. Phys. 12 (2010) 1982.
[24] A.W. Taylor, F.L. Qiu, I.J. Villar-Garcia, P. Licence, Chem. Commun. (2009) 5817.
[25] D. Weingarth, A. Foelske-Schmitz, A. Wokaun, R. Kötz, Electrochemistry Communications (2011) doi:10.1016/j.elecom.2011.03.027.

[26] R. Wibowo, L. Aldous, S.E.W. Jones, R.G. Compton, Chem. Phys. Lett. 492 (2010) 276.
[27] R. Wibowo, L. Aldous, E.I. Rogers, S.E.W. Jones, R.G. Compton, J. Phys. Chem. C 114 (2010) 3618.
[28] R. Wibowo, S.E.W. Jones, R.G. Compton, J. Chem. Eng. Data 55 (2010) 1374.
[29] R. Wibowo, S.E.W. Jones, R.G. Compton, J. Phys. Chem. B 113 (2009) 12293.
[30] H.E. Park, C.H. Hong, W.Y. Yoon, J. Power Sources 178 (2008) 765.
[31] D.R. MacFarlane, P. Meakin, J. Sun, N. Amini, M. Forsyth, J. Phys. Chem. B 103 (1999) 4164.
[32] M.E. Hyde, C.E. Banks, R.G. Compton, Electroanalysis 16 (2004) 345.
[33] S.H. Lee, J.C. Rasaiah, J. Phys. Chem. 100 (1996) 1420.
[34] S. Li, E.T. Kang, K.G. Neoh, Z.H. Ma, K.L. Tan, W. Huang, Appl. Surf. Sci. 181 (2001) 201.